Reconfigurable Intelligent Surface assisted massive MIMO systems based on phase shift optimization

Xuemei Bai[1*], Congcong Hou[1], Chenjie Zhang[1], and Hanping Hu[2]

[1] School of Electronics and Information Engineering, Changchun University of Science and Technology,
Changchun, 130022, Jilin, China
[e-mail: baixm@cust.edu.cn, 2022100852@mails.cust.edu.cn, custzcj@163.com]
[2] School of Science and Technology, Changchun University of Science and Technology,
Changchun, 130022, Jilin, China
[e-mail: hhp@cust.edu.cn]
[*]Corresponding author: Xuemei Bai

Abstract

Reconfigurable Intelligent Surface (RIS) is an innovative technique to precisely control the phase of incident signals with the help of low-cost passive reflective elements. It shows excellent potential in the sixth generation of mobile communication systems, which not only extends wireless coverage but also boosts channel capacity. Considering that multipath propagation and a high number of antennas are involved in RIS in assisted mega multiple-input multiple-output (MIMO) systems, it suffers from severe channel fading and multipath effects, which in turn lead to signal instability and degradation of transmission performance. To overcome this obstacle, this essay suggests an improved gradient optimization algorithm to dynamically and optimally adjust the phase of the reflective elements to counteract channel fading and multipath effects as a strategy. In order to overcome the optimization problem of falling into local minima, this paper proposes an adaptive learning rate algorithm based on Adagrad improvement, which searches for the global optimal solution more efficiently and improves the robustness of the optimization algorithm. The suggested technique helps to enhance the estimate of channel efficiency of RIS-assisted large MIMO systems, according to simulation results.

1. Introduction

$\mathbf{W}$ith 5G networks developing so quickly, there are increasing demands on the performance and capacity of wireless communication systems. Massive MIMO systems have attracted extensive research interest as a technique for spatial multiplexing through the application of several antennas, which significantly improves communication system performance, such as signal transmission efficiency and reliability [2,3]. Compared to 5G networks, 6G networks have higher requirements for performance metrics such as system saving energy, speed of transmission, dependability, and lag [1].

Reconfigurable Intelligent Surface (RIS) has emerged as a revolutionary concept in the past few years of wireless communication technology [4-11]. It is made up of several controllable inert tiny reflective elements. The values of the reflection coefficients of the reflective elements can be intelligently adjusted by programmable controllers, allowing the reflected signals to be propagated in a desired manner to the intended receivers. This makes the wireless environment controllable and programmable, enabling effective adjustment of the signal's transmission direction and enhancement of the signal's coverage, thus improving the functionality of the communication system. RIS is a more energy-efficient and cost-effective technology compared to existing amplify-and-forward relay-assisted communications [12-15].

Since RIS has the characteristics of low power consumption, flexible installation, can meet the requirements of future green communication, and has the sustainable development ability to cope with the growing number of users and applications, numerous academics both domestically and internationally have paid much attention to its development and conducted research in many aspects. In the research of channels estimate in mobile communications supported by RIS:

The authors in [16] propose a least squares-based algorithm for channel estimation for single RIS and dual RIS-assisted MIMO systems, and the outcomes of the simulation indicate that the dual RIS system enhances the channel estimation accuracy while reducing the training overhead. The authors in [17] used triangular inequality and successive convex approximation (SCA) methods to jointly optimize the phase shift of RIS elements in a multiple-input single-output (MISO) system, and the simulation results showed that the joint optimization resulted in a significant improvement in energy efficiency. The proposed optimized method demonstrates a 10.3% enhancement over the conventional Statistical Channel State Information (SCSI) algorithm. A technique based on least squares and alternating least squares decomposition was presented by the authors in [18] for RIS-assisted multiuser MISO systems' channel estimation, and the outcomes of the simulation indicate that the performance of the provided approach is improved in terms of initialization of the random channel matrix. The authors in [19] compared the performance of the minimum variance unbiased and minimum mean square error estimators in a MISO system with a RIS-assisted single user, and the numerical results showed that the minimum mean square error provided an improvement of more than 10 dB compared to the minimum variance unbiased estimator. The authors in [20] formulated a model of an RIS-assisted multiuser communication system considering blocking RIS and proposed a variational bayesian-based channel estimation algorithm that improves the robustness of the RIS blocking system while estimating the channel information and RIS assistance. The authors in [21] deployed a machine learning algorithm with three fully connected hidden layers for active and passive RIS elements to provide RIS-assisted channel estimation. The authors in [22] proposed a coverage maximization algorithm to solve the RIS placement optimization problem and finally obtained the optimal RIS direction. In literature [24], a hybrid solution for computing relatively small channel dimensions is suggested, and it

is illustrated using simulation that the proposed hybrid channel estimation method is significantly lower than other methods in terms of guide frequency overhead. Two sparse-aware RIS channel estimation schemes based on compressed sensing algorithms have been proposed in the literature [25], and experiments have shown that the schemes can adaptively form a beam toward the receiver to improve communication quality. The authors in [27] used a maximum likelihood estimator combined with a maximum correlation estimator to achieve an energy-efficient and computationally efficient beamforming alternative. The authors in [28] derive the downlink and reachable rates for multiuser massive MIMO systems in the Riel channel model and propose a particle swarm optimisation approach to solve the rate maximisation problem under RIS continuous and discrete phase shifts. The authors in [29] considered the effect of phase shift optimisation on maximisation and rate in RIS-assisted massive MIMO systems in the presence of transceiver hardware defects in the direct link.

With the release of the 6th generation mobile communications white paper, the problem of phase shift optimization for huge MIMO systems supported by RIS has received increasing attention [23]. In this piece of work, a phase optimization algorithm based on the combination of gradient descent method and adaptive learning rate is proposed for the RIS-assisted large-scale MIMO system with adaptive change of phase parameters to improve transmission efficiency and coverage area, and good experimental results are obtained. The following is a summary of this paper's primary contributions:

- In this work, based on the randomly generated transmit angle and signal arrival angle, by simulating the channel transmission process, the difference with the traditional method is that the fixed setting of parameters such as fading coefficients is discarded, and a random transmission channel model that is more in line with the practical needs is chosen. A rigorous mathematical framework and advanced probability distribution theory are used to ensure that the simulation results reflect the real signal transmission complexity in a highly controlled scenario. This innovative approach not only deepens the understanding of channel characteristics but also provides an accurate and reliable reference for future communication system design.
- In this paper, an approach based on an adaptive gradient optimization algorithm is proposed to provide support for performance optimization of large-scale systems with multiple inputs and multiple outputs (MIMO). The algorithm uses the gradient descent method to dynamically adjust the phase of the reflective elements to effectively attenuate interference factors such as channel fading and multipath effects. In addition, the introduction of the mechanism of adaptive learning rate aims to solve the problem that the gradient descent technique frequently encounters local minima when solving non-convex optimization issues, thus improving the accuracy of channel estimation.

The remainder of the document is explained below: The system model is described in Section 2. Section 3 explains the RIS phase shift optimization problem and leads to the method suggested in this article. Section 4 evaluates the performance of this paper's algorithm through convergence, computational complexity, normalized mean square error, BER, RIS size, and guide frequency overhead. Section 5 summarises the paper and indicates future directions.

2. System Models

In this study, we examine a transmission model for a massive MIMO system with RIS assistance in the downlink. It is comprised of k Users, an RIS with NL passive reflective elements, and a BS with NM antennas, as seen in **Fig. 1**.
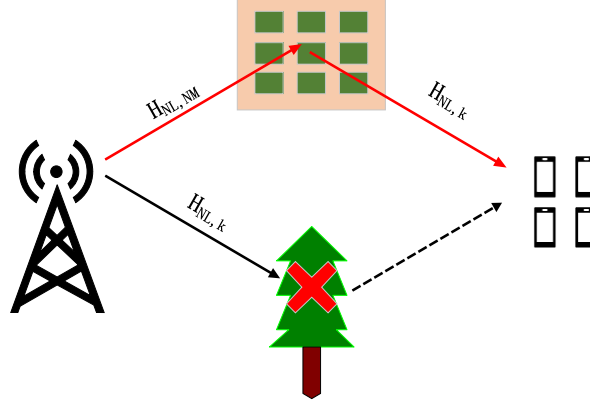
Fig. 1. Transmission scenario of RIS-assisted massive MIMO system

If the transmission scenario encounters the obstacle situation shown in **Fig. 1**, resulting in the BS side not being able to reach the Users side directly, only a cascade channel exists in the transmission scenario for the BS side to reflect to the Users side via the RIS. Let the antenna response vector $AoA_i \in C^{NL \times N_f}$ corresponding to each incidence angle and $AoD_i \in C^{NM \times N_f}$ corresponding to each outgoing angle, from the BS end to the RIS end, where NL denotes the RIS's number of reflecting elements, NM indicates how many antennas are there at the BS end, and N_f indicates the quantity of channels from the BS end to the RIS end,

$$AoA_i = e^{(-j\pi \sin(\theta_{nmAOA_i})*[0:NL-1])^T} \tag{1}$$

$$AoD_i = e^{(-j\pi \sin(\theta_{nmAOD_i})*[0:NM-1])^T} \tag{2}$$

where, $\theta_{nmAOA_i} \sim U(-\frac{\pi}{2},\frac{\pi}{2})$, $\theta_{nmAOD_i} \sim U(-\frac{\pi}{2},\frac{\pi}{2})$, denotes the BS end to the RIS end in using the probability distribution theory to generate a random incidence angle, and similarly, denotes the BS end to the RIS end in using the probability distribution theory to generate a random outgoing angle; the superscript T denotes the transpose operator.

Denote by F the channel's matrices between the BS and RIS sides,

$$F = \sum_{i=1}^{N_f} \alpha_i (AoA_i \otimes AoD_i) \tag{3}$$

where, N_f denotes the number of channels from the BS end to the RIS end; α_i denotes the fading coefficient of the i-th path; AoA_i denotes the antenna response vector corresponding to the i-th incidence angle from the BS end to the RIS end; AoD_i denotes the antenna response vector corresponding to the i-th outgoing angle from the BS end to the RIS end; and $\otimes$ denotes the tensor product.

Similarly, denoting the channel matrix from the RIS side to the Users side by H_k,

$$H_k = \sum_{i=1}^{N_{hk}} \alpha_i \ AoD_k^{(i)} \tag{4}$$

where, N_{hk} denotes the number of channels from the RIS end to the Users end; α_i denotes the fading coefficient of the i-th path; $AoD_k^{(i)}$ denotes the antenna response vector $AoD_k \in C^{NL \times N_{hk}}$ corresponding to the signal outgoing angle of the i-th user from the RIS end to the Users end,

$$AoD_k = e^{(-j\pi \sin(\theta_{Users})*[0:NL-1])^T} \tag{5}$$

where, $\theta_{Users} \sim U(-\frac{\pi}{2},\frac{\pi}{2})$, θ_{Users} denotes that the RIS end to the Users end at $(-\frac{\pi}{2},$

$\frac{\pi}{2}$）generates a random angle of incidence for each user using probability distribution theory; the operator for transposing is indicated by the superscript T.

The channel matrix for user k is denoted G_k and consists of the channels matrices F connecting the RIS and BS sides and the channels matrices H_k from the RIS side to the Users side, denoted as,

$$G_k = \text{diag}((H_k)^H) * F \tag{6}$$

where $\text{diag}((H_k)^H)$ is denoted as being a diagonal matrices whose diagonal elements are components of $(H_k)^H$; the superscript H is denoted as the conjugate transpose operator.

The noise matrix during channel transmission is $N_k \epsilon C^{NM \times N_{bpilot}}$,

$$N_{:, b, k} = \frac{U_{:, (N_{npilot} * (b-1)+1) : (N_{npilot} * b)} * \text{Userpilot}_{:, k}}{\sqrt{SNR} * N_{npilot}} \tag{7}$$

where, $N_{:, b, k} \in C^{NM * 1}$ represents the noise received by the BS antenna from User k symbolised out at the b-th lead frequency; $U_{:, (N_{npilot} * (b-1)+1) : (N_{npilot} * b)}$ represents the extraction of the noise submatrix associated with the current leading frequency symbol b; N_{npilot} denotes the number of guided frequencies sent by each User; $\text{Userpilot}_{:, k}$ denotes the pilot sequence sent by User k; $SNR = \frac{S}{N}$, S denotes the signal power, N denotes the noise power, and SNR denotes the signal-to-noise ratio; the $\sqrt{SNR} * N_{npilot}$ is to ensure that the variance of the noise matches a given sign-to-noise proportion; N_{npilot} is the length of the training sequence for each user. The U-matrix is denoted by,

$$U = \frac{1}{\sqrt{2}}(N_r + j * N_i) \tag{8}$$

where, $U \in C^{NM * (N_{npilot} * N_{bpilot})}$ denotes the complex Gaussian noise matrix with mean 0 variance 1; N_r and N_i denote the real and imaginary parts of the complex Gaussian noise matrix, respectively; Each element in N_r and N_i is a random variable generated independently from a normal distribution with mean 0 variance 1; $\frac{1}{\sqrt{2}}$ is to ensure that both the real and imaginary parts of each complex noise element have a variance of 0.5 so that the entire complex noise element has a variance of 1.

Joining Eq. (6) and Eq. (7) yields the received signal Y_k, denoted as,

$$Y_k = G_k^H * V + N_k \tag{9}$$

where, Y_k represents the Users k 's received signal matrix; G_k is the channel matrix of Users k, which consists of the matrix of channels F from the BS side to the RIS side and the channel matrix H_k from the RIS side to the Users side; the combination of the coefficients for reflection at the RIS end is indicated by V; N_k is the noise matrix; V denotes the matrix of reflection coefficients at the RIS end,

$$V = \frac{1}{\sqrt{2}}(N(0,1) + j * N(0,1)) \tag{10}$$

where, $N(0,1)$ denotes the generation of an independently and identically distributed standard normal random variable with mean 0 and variance 1; j denotes an imaginary unit; and $\frac{1}{\sqrt{2}}$ is to ensure that the variance of the elements of V is 1 so that it is a standard complex Gaussian random variable.

3. Phase-shift Optimization Problems

In this research, we examine how accurate channel state data is in multiuser MIMO systems

with RIS assistance, and express the precision of the channel state data in terms of the Normalised Mean Square Error (NMSE), which is able to be stated as,

$$\text{NMSE} = \frac{\text{Trace}((\hat{G}\text{-}G)^{H}(\hat{G}\text{-}G))}{\text{Trace}(G^{H}\text{-}G)} \tag{11}$$

where, $\hat{G}$ denotes the estimated channel matrix; G denotes the theoretical channel matrix.

3.1 Optimization Algorithms

In order to focus the signal energy in a specific direction and improve the energy efficiency and quality of signal reception. In this paper, we consider the introduction of optimization algorithms to change the phase of the reflective elements of the RIS, the common optimization algorithms are exhaustive, Newton's method, Lagrange multiplier, and gradient descent, the comparison **Table 1** of these optimization algorithms is given as follows,

Table 1. Comparison of optimization algorithms

Algorithms	Advantages	Disadvantages
Exhaustive indexing algorithm	Simple and easy to implement	High computational complexity, growing exponentially with coefficient size
Newton's method	Applicable to secondary optimization issues	High computational complexity, especially in large-scale problems
Lagrange multiplication	For RIS phase-shift optimization problems with constraints	Need to introduce Lagrange multipliers to deal with constraints, increasing the complexity of the problem; solving some errors
gradient descent method	Easy to implement, faster convergence	For non-convex optimization problems, it is easy to fall into local minima

The method used in this paper for the gradient descent approach is used to solve the RIS phase-shift problem of optimization, which is a very versatile optimization algorithm that makes the objective function gradually converge to a minimum by repeatedly adjusting the values of the parameters [30, 33]. Searching in the direction of the goal function's gradient is the fundamental idea behind this approach.

The specific steps for the implementation of the gradient descent method are as follows:

- Determine the objective function: suppose there is an objective function $J(\theta)$, where θ is a vector of parameters waiting to be optimized.
- Determine the gradient vector: the gradient (or derivative) of the objective function $\nabla J(\theta)$ is a vector that holds the goal function's partial derivatives with regard to each parameter. The direction of the gradient is the direction in which the function rises fastest at the current point.
- Parameter update: The rule for parameter update is usually $\theta = \theta - \alpha*\nabla J(\theta)$.

In this paper, when using the gradient descent method for optimization, the aim is to compute the correlation when the leading frequency sequence is "LISpilot", so the intended purpose is the correlation value of J(LISpilot). The gradient algorithm, on the other hand, is a partial derivative of the objective function, and for each derivative sequence element LISpilot_i, the gradient is computed as,

$$\frac{\partial J}{\partial \text{LISpilot}_i} = \text{-LISpilot}_i + D_r * (D_r^{H} * \text{LISpilot}_i) \tag{12}$$

where, D_r^H is the conjugate transpose of the transfer matrix D_r. D_r is a matrix of $NL \times Gr$; LISpilot refers to the lead frequency sequence.

The gradient update is expressed as follows,

$$\text{LISpilot}_i = \text{LISpilot}_i - \alpha * \frac{\partial J}{\partial \text{LISpilot}_i} \tag{13}$$

where α is a random parameter, specifically represented as model parameters for adaptive learning rate.

3.2 Adaptive Learning Rates

The adaptive learning rate used in this paper is capable of dynamically adjusting the size of the learning rate for different parameter updates based on their historical gradients [31]. This algorithm's fundamental concept is to utilize a higher learning rate for parameters that occur seldom and a lower learning rate for parameters that occur frequently. This adaptivity helps to better handle sparse features and frequently occurring features during training.

The specific steps for the implementation of the adaptive learning rate are as follows:

- Cumulative gradient squared term: the core idea of adaptive learning rate is to maintain a cumulative gradient squared term for each parameter. For each parameter wi, the algorithm maintains a cumulative squared gradient term G_i with an initial value of 0. Denoted as,

$$G_i = G_i + (\nabla J(wi))^2 \tag{14}$$

where $\nabla J(wi)$ denotes the gradient of the loss function with respect to the parameter wi.

- Modification of the learning rate: The rules for updating the learning rate are as follows:

$$\text{learning rate} = \frac{\text{Initial learning rate}}{\sqrt{G_i + \epsilon}} \tag{15}$$

where, ϵ is a minuscule constant, mostly to prevent division by zero mistakes.

- Parameter update: The final parameter update rule is:

$$wi = wi - \text{learning rate} \times \nabla J(wi) \tag{16}$$

where $\nabla J(wi)$ denotes the gradient of the loss function concerning the parameter wi.

In this paper, during phase-shift optimization using adaptive learning rate-assisted gradient descent, the square of the gradient is accumulated in each iteration, denoted as,

$$G_t = G_{t-1} + g_t^2 \tag{17}$$

where G_t is the cumulative sum of squares of the gradients up to the tth iteration; similarly, G_{t-1} is the cumulative sum of squares of the gradients up to the $t-1$st iteration; and g_t denotes the gradient vector of the tth iteration.

Adjustment of the learning rate can be performed using equation (17), which can be expressed as,

$$\eta_t = \frac{\eta_0}{\sqrt{G_t + \in}} \tag{18}$$

where, η_t denotes the value of the learning rate after the tth iteration; η_0 denotes the initial learning rate; and ϵ is a very small constant, mainly to avoid division by zero errors.

The parameter update based on the results obtained from Eq. (18) can be expressed

as,

$$\theta = \theta - \eta_t \times g_t \tag{19}$$

where, θ is the model parameter to be updated, refers to the unknown number α in the gradient descent method.

3.3 Improved Gradient Descent

It can be seen through Eq. (12) and Eq. (13) that the issue at hand pertains to non-convex optimization, and the gradient descent method is easy to fall into the local minima for solving the non-convex issue, and it is not possible to get the global minimum, so an improved gradient descent method is proposed as gradient descent method and adaptive learning rate (GDALR). the GDALR algorithm is to introduce the result of Eq. (19) into Eq. (13) instead of α. It can adaptively modify the parameter values according to the gradient values, which can better solve the present convex optimization problem, so that the probability of falling into the local minima is reduced, and the channel state information's correctness has increased.

The GDALR algorithm is implemented in the following specific flow:

Algorithm:	GDALR algorithm
Input:	Get parameters such as receive matrix, transmit matrix, length, etc. from the structure system.
	Parameters such as num_iterations, initial_learning_rate, etc.
Output:	**LISpilot0**
1 :	**If** rank(LISpilot)≥N_bpilot **then**
2 :	**for** iter = 1:num_iterations
3 :	Calculate LISpilot correlation
4 :	Calculate the gradient according to equation (12)
5 :	Adaptive learning rate adjustment according to Eqs. (17) and (18)
6 :	Updating the guide frequency sequence
7 :	Recalculating correlations
8 :	**if** new_cur > cur LISpilot = LISpilot0; **break;** **end**
9 :	**Output LISpilot0**

● The first step is to initialize the LISpilot and ensure that the generated LISpilot is full rank.
● The second step is to update the iterative optimization process in which the phase is optimized using a modified gradient descent method, i.e., the GDALR algorithm, and then the correlation of the new lead frequency sequence generated after the GDALR algorithm is calculated based on the Muturalance_correlance work.
● The subsequent action is to judge the size of the newly generated correlation value new_cur and the original correlation value cur, and if new_cur > cur, then the assignment is made; otherwise, the calculation is repeated.
● Repeat steps 2, 3, 4, 5, 6, 7, and 8 in the above table until the conditions of step 8

are met, then the loop will be jumped out, the assignment will be made and LISpilot0 will be output.

4. Simulation Results Analysis

To ensure that validation of the effectiveness of the improved gradient descent algorithm (GDALR algorithm) in enhancing the accuracy of the acquired channel state information in the system simulation of channel estimation for RIS-assisted massive MIMO systems. This paper further validates the ability of phase shift optimization without RIS and with sequence optimization about the precision of the channel status data collected for this system. Simulations are carried out using Matlab software to acquire the information about the channel status and the estimation effect is evaluated by convergence, computational complexity, normalized mean square error, bit error rate, pilot overhead ratio, and RIS size.

4.1 Simulation Settings

In this paper, we assume that the quantity of transmitting antennas at the BS is NM = 4, the quantity of passive reflective elements at the RIS is NL = 256, and the quantity of antennas at the service Users's end is k = 4. Number of each subframe ParameterB = 8, 16, 24, 40, 72, 128, 256. The guide sequence is a discrete fourier transform (DFT) matrix, the angle of incidence from the BS end to the RIS end is θ_{nmAOA_i}, as well as the angle of departure between the Users end and the RIS end is θ_{nmAOD_i}. The incidence angle and the departure angle are random values of an angle in $(-\frac{\pi}{2}, \frac{\pi}{2})$. Unless otherwise stated, the number of conduction subcarriers at the end of each user is fixed at 16, i.e., the conduction overhead is N_p/ParameterBmax = 6.25%. For LS, LS-Sequence, and LS-GDALR, the maximum number of iterations T = 100. In addition, for fairness, newer pilot modes, such as the uniform pilot scheme and the random pilot scheme, for RIS-assisted orthogonal frequency division multiplexing (OFDM) systems in [26], are considered as a baseline for comparison tests. All illustrations shown are obtained by averaging over 500 Monte Carlo experiments. The algorithms in this paper are described as follows, along with the comparison algorithms in the simulation results.

- EWOA-CCS:The WOA algorithm refers to the whale algorithm, EWOA is an enhanced whale algorithm proposed based on the whale algorithm, which combines the press coding scheme (CCS) in the enhanced whale algorithm, called EWOA-CCS.
- CS-EWOA: Since the pilot allocation in the framework of compressed sensing (CS) has a significant impact on the channel estimation performance, it is proposed to combine the enhanced whale algorithm (EWOA) with compressed sensing (CS), called CS-EWOA.
- EWOA-SOCP: In order to solve the non-convex optimization problem, the use of second-order cone programming with the augmented whale algorithm, called EWOA-SOCP, is proposed.
- Uniform Scheme: represents the uniform pilot scheme (i.e., uniform position and average power) from the literature [26].
- Random Scheme: represents the random pilot scheme (i.e., random position and average power) from the literature [26].

- LS: The sparse signal is first compressed by compressed sensing (CS), and then the channel estimation is solved using the LS estimator.
- LS-Seqence: a sequence optimization algorithm is added to the LS algorithm solution, followed by a channel estimation solution.
- LS-GDALR: The proposed GDALR optimization algorithm is added to the LS algorithm solution and finally the channel estimation solution is performed.

4.2 Comparison of Convergence

This subsection looks into how the number of iterations with various algorithms changes in relation to the change in the fitness value. From **Fig. 2**, it is evident that when there are more than 50 iterations, the fitness values of EWOA-CCS, CS-EWOA, and EWOA-SOCP are much greater than those of LS-GDALR, LS, and LS-Seqence [34]. In contrast, the three LS-based algorithms have better fitness values when the number of iterations is larger, but the fitness values obtained by LS-Seqence oscillate between [0.1,0.9] with larger fluctuations; the fluctuations of the fitness values of LS range between [0.05,0.42], which is more stable than that of the LS-Seqence method that can obtain a more stable fitness value, but in the case of the number of iterations less than 20 the fitness value obtained by LS algorithm is larger than the fitness value of the three EWOA-based methods; the fitness value obtained by LS-GDALR algorithm oscillates between [0.04,0.2], compared with less fluctuation, and the fitness value obtained is the most stable, and it can also be seen from the figure that LS-GDALR algorithm outperforms the other algorithms in terms of convergence accuracy of fitness value.
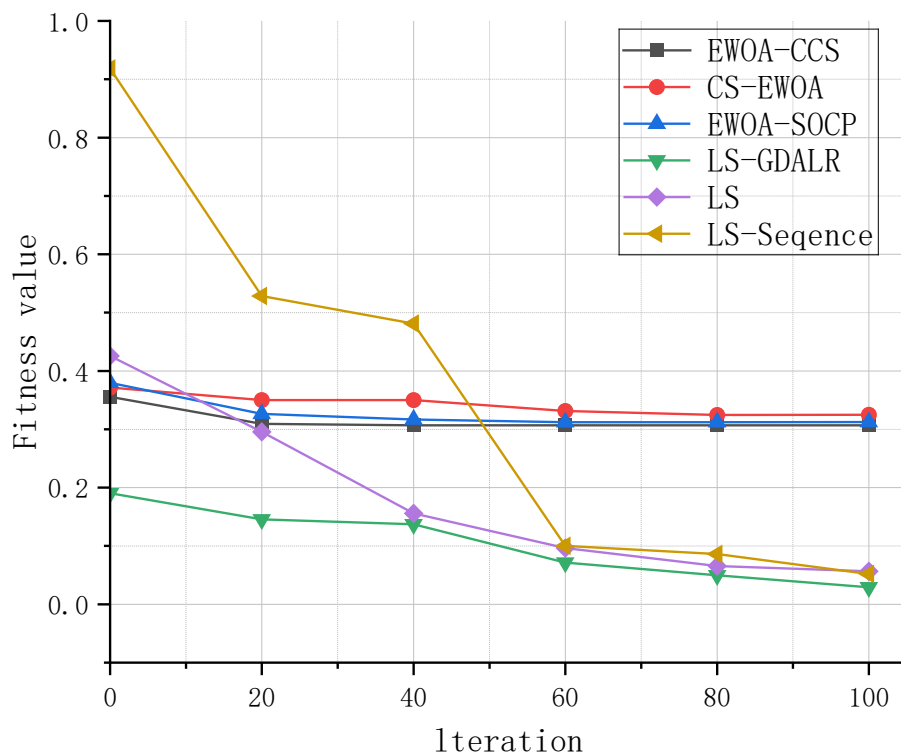

Fig. 2. Algorithm convergence comparison

4.3 Comparison of Computational Complexity

To be fair, the method's computational complexity as presented in this paper is analyzed by considering the same amount of transmitting antennas NM at the BS end, the number of subframes, and the quantity of antennas k at the serving Users end. From **Fig. 3**, It is evident that when there are more than or equal to 40 subframes, the computational complexity of the three LS-based methods remains consistent and lies between [10^4,10^5]. From the subgraphs in **Fig. 3**, observations show that when there are fewer than forty subframes, the complexity obtained from the computation of the LS method and the LS-Seqence method remains the same, while the complexity obtained by the LS-GDALR algorithm is about 0.1 smaller than that of the other two methods. Overall, the LS-GDALR algorithm is considered to have low computational complexity and reduces the cost of computation.
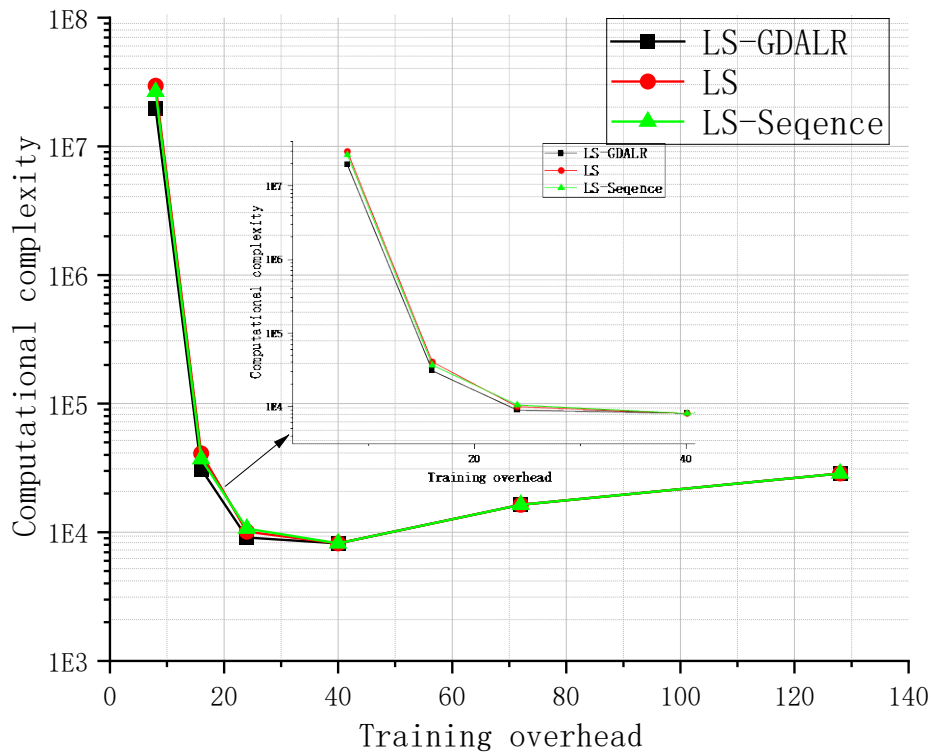

Fig. 3. Comparison of computational complexity

4.4 Performance Comparison of NMSE and BER

Since this paper investigates RIS-assisted massive MIMO systems, only the bit error rate (BER) versus the cascaded channel's signal-to-noise ratio (SNR) and the normalized mean square error (NMSE) versus that ratio are taken into consideration. For cascaded channels, **Fig. 4** shows the normalized mean square error (NMSE) vs signal-to-noise ratio (SNR). From the figure, it is evident that the normalized mean square error of each algorithm decreases as the SNR increases. However, it can be seen that the three LS-based algorithms mentioned in this paper perform superior to the three CS-based algorithms proposed in the literature [8], the uniformly inserted frequency-guided algorithm in [26], and the stochastic algorithms, which yield lower values of the normalized mean square error. For example, at 30 dB, the LS algorithm's normalized mean square error is reduced by $2.019*10^{-4}$ compared to the inaccuracy of the normalized mean square obtained by the EWOA-CCS algorithm; The normalized mean square error of the LS-Sequence algorithm is reduced by $2.022*10^{-4}$ compared to the inaccuracy of the normalized mean square obtained by the EWOA-CCS algorithm; The inaccuracy of the normalized mean square of the LS-GDALR algorithm is reduced by $2.022*10^{-4}$ compared to the error value obtained by the EWOA-CCS algorithm [34]. Although, at 30 dB, the LS-Sequence algorithm and LS-GDALR algorithm have the same difference in normalized mean square error reduction as the EWOA-CCS algorithm, the values of normalized mean square error for the LS-Sequence algorithm and the LS-GDALR algorithm at this SNR are $1.47*10^{-7}$ and $1.2*10^{-7}$ respectively. So, the LS-GDALR algorithm has better channel estimation performance.

The link between signal noise ratio (SNR) and bit error rate (BER) in a cascaded channel is shown in **Fig. 5(a)**. From the figure, it is evident that the BER value of each algorithm decreases as the SNR increases. However, it can be seen from the figure that the LS-based algorithm proposed in this paper has a smaller value of BER when the SNR rises, indicating the better performance of the LS-based algorithm, which is in line with the normalized mean square error performance in **Fig. 4**. For example, at 30 dB, the BER value of the LS algorithm is $1.089*10^{-4}$ less than the Prefect CSI's BER value; the BER value of the LS-Sequence algorithm is $1.094*10^{-4}$ smaller than the BER value of Prefect CSI; the BER value of the LS-GDALR algorithm is $1.104*10^{-4}$ smaller than the BER value of Prefect CSI. That is challenging to distinguish the BER output of the three LS-based algorithms from **Fig. 5(a)**, so the BER effectiveness of the LS algorithm, LS-Seqence algorithm, and LS-GDALR algorithm is represented in **Fig. 5(b)**, and It's evident from the graph in **(b)** as well as the sub-graphs of the graph in **(b)**, that the BER performance of the three LS-based algorithms is the same only when the SNR is equal to 20 dB, and the BER values obtained from the LS-GDALR algorithm is less than that obtained from the LS-Seqence algorithm and LS algorithm for the other values of the SNR and the LS algorithm gives better performance.
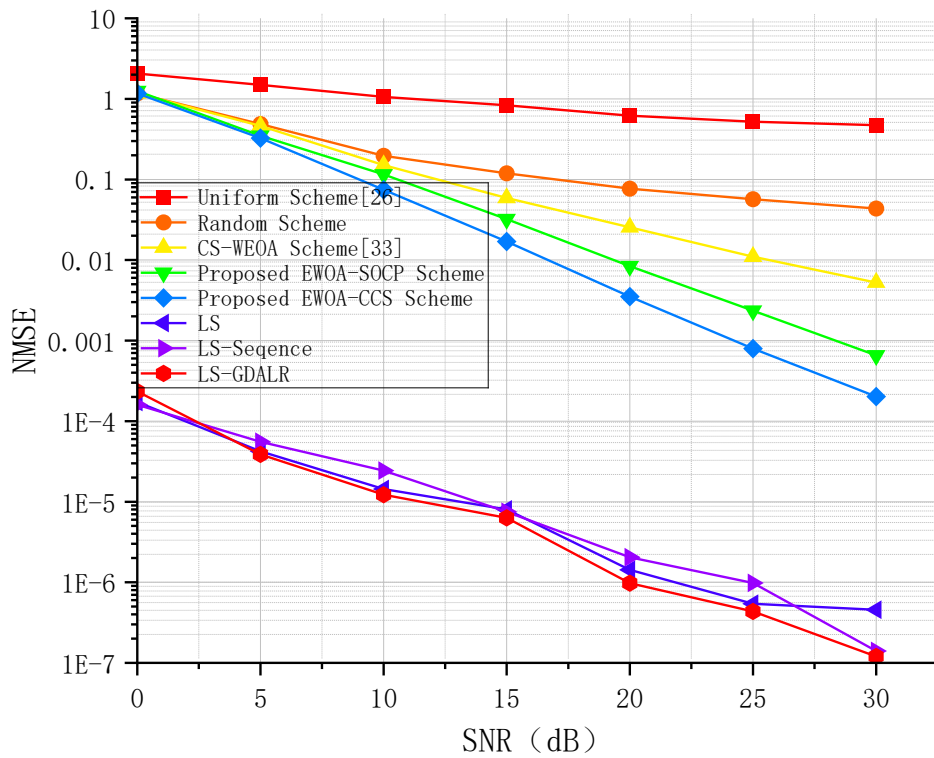
Fig. 4. Normalised mean square error results for different signal-to-noise ratios
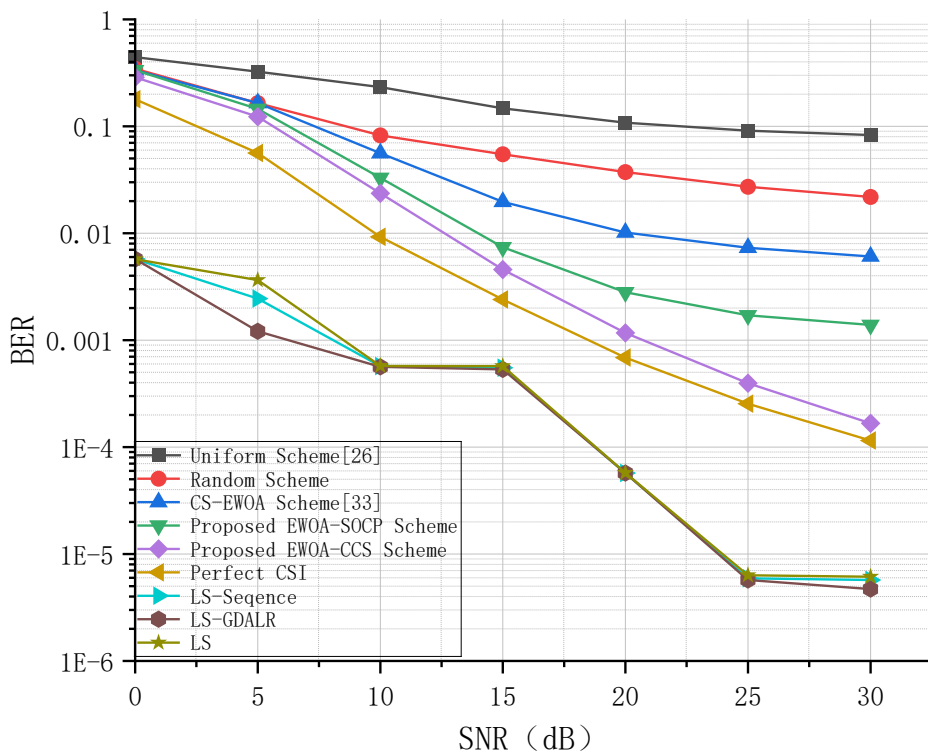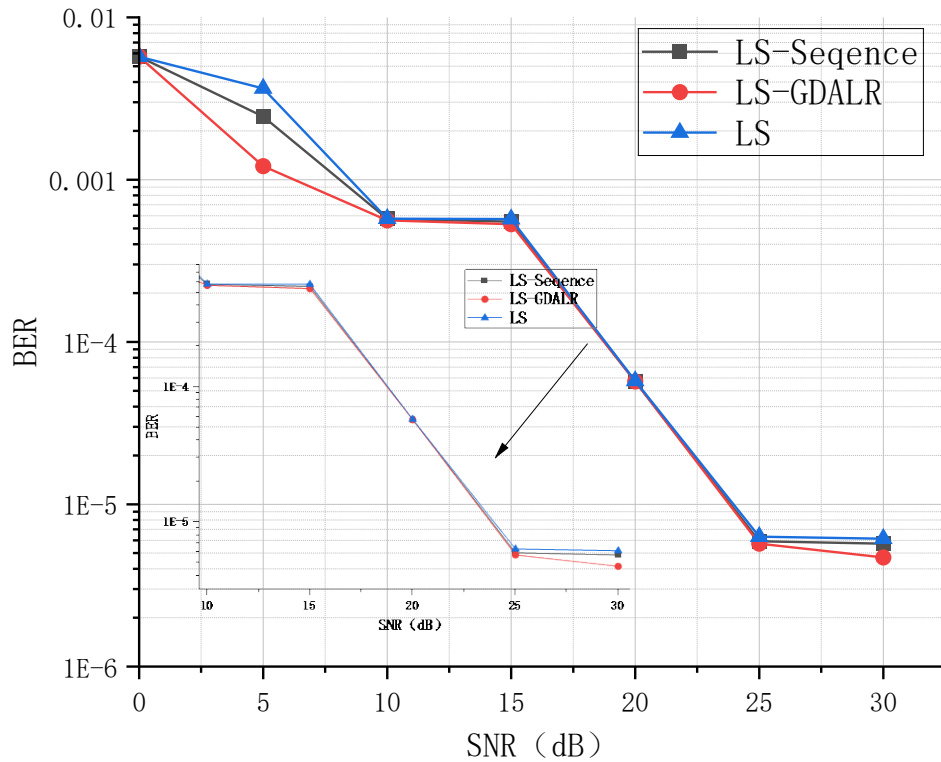

Fig. 5(a). Results of BER with SNR

Fig. 5(b). Results of LS-based algorithm with BER for SNR variation

4.5 NMSE and BER Performance Comparison for Various RIS

This subsection examines how the normalized mean square error and BER performance of compressed channel estimation are affected by varying the amount of RIS reflection elements. The settings for the simulation are as follows: $P_{max} = 60$dBm，$N = 128, N_p = 16$，NL = 8，64，256, respectively. As shown in **Fig. 6** the resultant plots of normalized mean square error obtained for a different number of RIS reflection elements with increasing SNR, as the quantity of RIS reflection elements M increases from 8 to M=64, most of the algorithms show a gradual decrease in normalized mean square error with increasing SNR, only the LS algorithm shows a gradual increase in the normalized mean square error or keeps it unchanged with the increase in the SNR, so based on which LS-Seqence algorithm and LS-GDALR algorithm have been proposed. From the figure, it can be observed that both LS-Seqence algorithm and LS-GDALR algorithm get better results as the SNR increases, e.g., at M=8, SNR=30dB, LS-Seqence algorithm and LS-GDALR algorithm reduce by 0.1881 and 0.1883 compared to EWOA-CCS algorithm; at M=64, the SNR=30dB, the LS-GDALR algorithm reduces 0.0008 than the EWOA-CCS algorithm [34]. The estimation performance of most algorithms decreases when M is increased from 64 to 256. This effect is due to the fact that, in real life, when the value of M is large, the resulting channel becomes more complex, so the accuracy of the channel estimation decreases. Based on the illustration, one can see that the LS-GDALR algorithm is gradually improving the channel estimation accuracy as the normalized mean square error value is decreasing with increasing M and SNR.

As shown in **Fig. 7** the resultant graphs of BER obtained for varying quantities of RIS reflection elements with increasing SNR, the BER of all the algorithms decreases gradually with increasing SNR as the reflection elements of RIS go from 8 to 64 and one can see that the LS-based method suggested in this work performs better than EWOA based algorithm for channel estimation, e.g., the LS algorithm reduces the BER than EWOA-CCS algorithm by $1.839*10^{-4}$ for M=64,SNR=30dB; The LS-Sequence algorithm is $1.851*10^{-4}$ less than the EWOA-CCS algorithm; The LS-GDALR algorithm is $1.865*10^{-4}$ less than the EWOA-CCS algorithm. By the time M grows to 256 from 64, the performance of the channel estimation of the EWOA-based algorithm decreases, while the channel estimation performance of the LS-based algorithm proposed in this paper improves, and the graphic shows that the LS-GDALR algorithm performs better in channel estimation than the other two techniques.
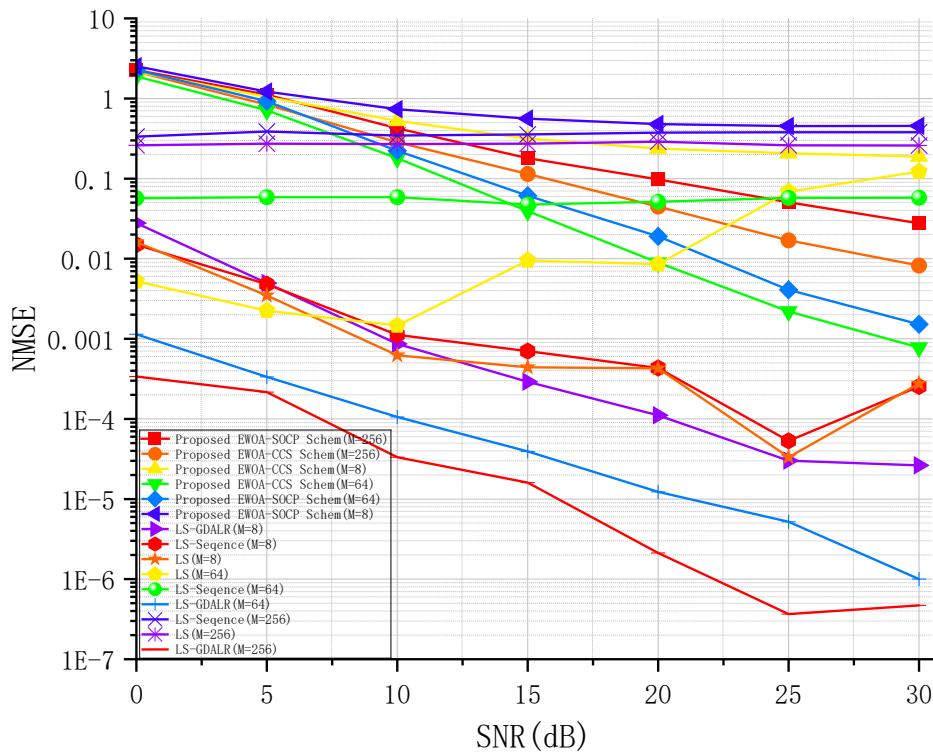

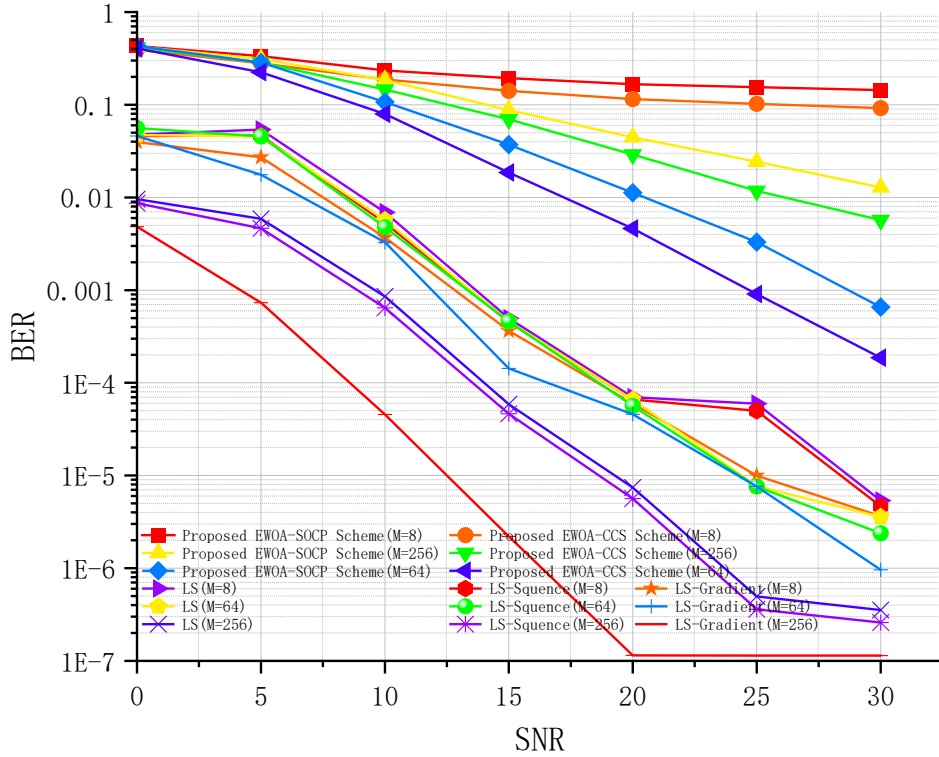**Fig. 6.** Normalised mean square error results with different RIS reflection elements

Fig. 7. BER results with different RIS reflection elements

4.6 Performance Comparison of Pilot Overhead Ratio

It is evident from **Fig. 4** and **Fig. 5** that the LS-based algorithm proposed in this paper obtains better results in relation to normalized mean square error and BER when the same number of leads $N_p = 16$ is used. This subsection builds on this foundation and **Fig. 8** compares the effect on the normalized mean square error values for different lead frequency overhead ratios. As shown in the figure, the normalized mean square error of all the algorithms decreases accordingly as the lead frequency overhead ratio increases. The algorithm proposed in this paper requires fewer guide frequencies than the EWOA-based algorithm to achieve the same normalized mean square error. For example, when the normalized mean square error is between $[10^{-4}, 10^{-3}]$, the EWOA-CCS algorithm requires a lead ratio of 12.5%, while the three LS-based algorithms proposed in this paper require lead ratios between $[4\%, 5\%]$ [34]. These results demonstrate that the suggested technique may successfully lower the frequency conduction overhead and further minimize computing costs, improving spectral efficiency.
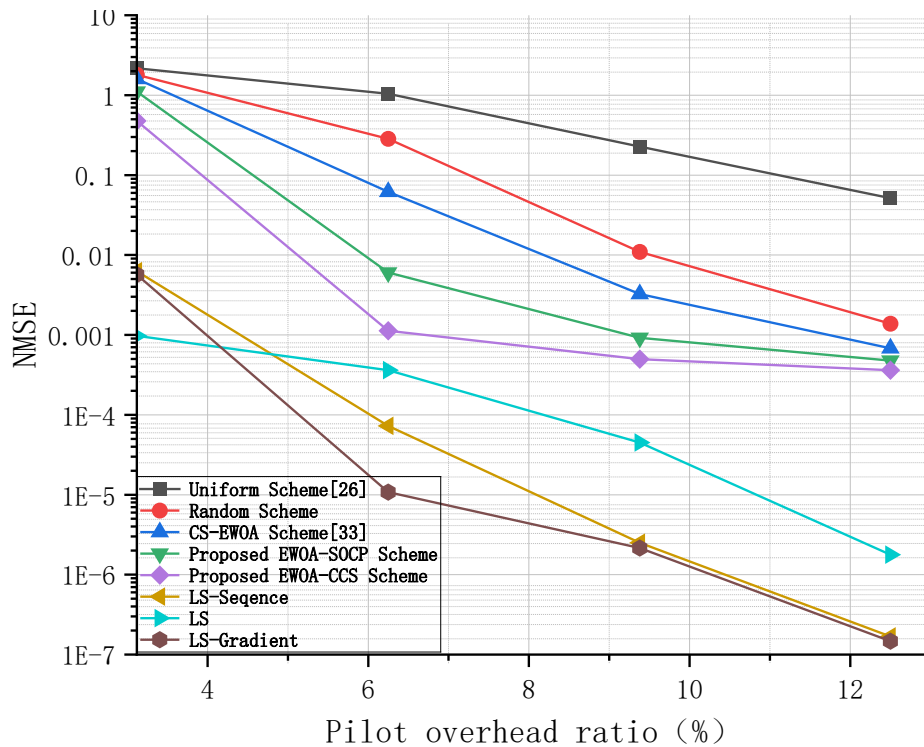
Fig. 8. Pilot overhead ratio results

5. Conclusions and Future Work

In this paper, an optimization method for RIS-assisted massive MIMO systems is investigated and an adaptive gradient-based optimization algorithm (GDALR algorithm) is proposed to bolster the channel estimation's correctness. Firstly, the results of channel estimation without the optimization method are presented; based on this, the RIS phase-shift optimization method with sequence optimization is suggested for the estimate of channels, and the results of the normalized mean square error at different signal-to-noise ratios show that the results of channel estimation without the addition of the optimization method are improved by $3.08*10^{-7}$ compared to the results of channel estimation with sequence optimization; Based on this, an adaptive gradient-based optimization algorithm (GDALR algorithm) is proposed for channel estimation, and the GDALR algorithm improves the channel estimation results over the sequence optimization algorithm by $2.7*10^{-8}$. According to simulation results, the suggested approach performs better than the current schemes in terms of computational complexity, BER, RIS size, convergence, normalized mean square error, and pilot overhead ratio, all of which can obtain more accurate channel state information.

Future directions for research:

- When studying RIS-assisted massive MIMO systems, the computational complexity can be reduced while ensuring accurate channel state information;
- Study of the dual RIS-assisted massive MIMO system problem.

References

[1] J. Zong, Y. Liu, H. Liu, Q. Wang, and P. Chen, "6G Cell-Free Network Architecture," in *Proc. of 2022 IEEE 2nd International Conference on Electronic Technology, Communication and Information (ICETCI)*, pp.421-425, 2022. Article (CrossRef Link)

[2] Z. Ding and H. V. Poor, "A Simple Design of IRS-NOMA Transmission," *IEEE Communications Letters*, vol.24, no.5, pp.1119-1123, May 2020. Article (CrossRef Link)

[3] G. Zhou, C. Pan, H. Ren, and K. Wang, "Channel Estimation for RIS-Aided Millimeter-Wave Massive MIMO Systems : (Invited Paper)," in *Proc. of 55th Asilomar Conference on Signals, Systems, and Computers*, pp.698-703, 2021. Article (CrossRef Link)

[4] S. Liu, R. Liu, M. Li, Y. Liu, and Q. Liu, "Joint BS-RIS-User Association and Beamforming Design for RIS-Assisted Cellular Networks," *IEEE Transactions on Vehicular Technology*, vol.72, no.5, pp.6113-6128, May 2023. Article (CrossRef Link)

[5] F. -S. Tseng and T. -Y. Wang, "Reflection Design With LS Channel Estimation for RIS-enhanced OFDM Systems," in *Proc. of 2022 Thirteenth International Conference on Ubiquitous and Future Networks (ICUFN)*, pp.75-79, 2022. Article (CrossRef Link)

[6] C. Pan et al., "Intelligent Reflecting Surface Aided MIMO Broadcasting for Simultaneous Wireless Information and Power Transfer," *IEEE Journal on Selected Areas in Communications*, vol.38, no.8, pp.1719-1734, Aug. 2020. Article (CrossRef Link)

[7] J. An, C. Xu, L. Gan, and L. Hanzo, "Low-Complexity Channel Estimation and Passive Beamforming for RIS-Assisted MIMO Systems Relying on Discrete Phase Shifts," *IEEE Transactions on Communications*, vol.70, no.2, pp.1245-1260, Feb. 2022. Article (CrossRef Link)

[8] R. Jiang, Z. Fei, S. Huang, X. Wang, Q. Wu, and S. Ren, "Bivariate Pilot Optimization for Compressed Channel Estimation in RIS-Assisted Multiuser MISO-OFDM Systems," *IEEE Transactions on Vehicular Technology*, vol.72, no.7, pp.9115-9130, Jul. 2023. Article (CrossRef Link)

[9] C. Pan et al., "Reconfigurable Intelligent Surfaces for 6G Systems: Principles, Applications, and Research Directions," *IEEE Communications Magazine*, vol.59, no.6, pp.14-20, Jun. 2021. Article (CrossRef Link)

[10] C. Pan et al., "Multicell MIMO Communications Relying on Intelligent Reflecting Surfaces," *IEEE Transactions on Wireless Communications*, vol.19, no.8, pp.5218-5233, Aug. 2020. Article (CrossRef Link)

[11] S. Shen, B. Clerckx, and R. Murch, "Modeling and Architecture Design of Reconfigurable Intelligent Surfaces Using Scattering Parameter Network Analysis," *IEEE Transactions on Wireless Communications*, vol.21, no.2, pp.1229-1243, Feb. 2022. Article (CrossRef Link)

[12] X. Guan, Q. Wu, and R. Zhang, "Anchor-Assisted Channel Estimation for Intelligent Reflecting Surface Aided Multiuser Communication," *IEEE Transactions on Wireless Communications*, vol.21, no.6, pp.3764-3778, Jun. 2022. Article (CrossRef Link)

[13] Q. Wu and R. Zhang, "Intelligent Reflecting Surface Enhanced Wireless Network via Joint Active and Passive Beamforming," *IEEE Transactions on Wireless Communications*, vol.18, no.11, pp.5394-5409, Nov. 2019. Article(CrossRefLink)

[14] G. Zhou, C. Pan, H. Ren, K. Wang, and A. Nallanathan, "Intelligent Reflecting Surface Aided Multigroup Multicast MISO Communication Systems," *IEEE Transactions on Signal Processing*, vol.68, pp.3236-3251, 2020. Article (CrossRef Link)

[15] Q. Wu and R. Zhang, "Towards Smart and Reconfigurable Environment: Intelligent Reflecting Surface Aided Wireless Network," *IEEE Communications Magazine*, vol.58, no.1, pp.106-112, Jan. 2020. Article (CrossRef Link)

[16] K. Ardah, S. Gherekhloo, A. L. F. de Almeida and M. Haardt, "Double-RIS Versus Single-RIS Aided Systems: Tensor-Based Mimo Channel Estimation and Design Perspectives," in *Proc. of ICASSP 2022 - 2022 IEEE International Conference on Acoustics, Speech and Signal Processing (ICASSP)*, pp.5183-5187, 2022. Article (CrossRef Link)

[17] C. Yang, K. Yu and X. Yu, "Energy Efficiency Optimization for Distributed RIS-Assisted MISO System Based on Statistical CSI," in *Proc. of 2022 IEEE 22nd International Conference on Communication Technology (ICCT)*, pp.875-879, 2022. Article (CrossRef Link)

[18] C. Beldi, A. Dziri, F. Abdelkefi and H. Shaiek, "PARAFAC Decomposition based Channel Estimation for RIS-aided Multi-User MISO Wireless Communications," in *Proc. of 2023 International Wireless Communications and Mobile Computing (IWCMC)*, pp.1537-1542, 2023. Article (CrossRef Link)

[19] R. V. Şenyuva, "Channel Estimation for RIS aided MISO System," in *Proc. of 2023 31st Signal Processing and Communications Applications Conference (SIU)*, pp.1-4, 2023. Article (CrossRef Link)

[20] S. Ma, W. Shen, X. Gao, and J. An, "Robust Channel Estimation for RIS-Aided Millimeter-Wave System With RIS Blockage," *IEEE Transactions on Vehicular Technology*, vol.71, no.5, pp.5621-5626, May 2022. Article (CrossRef Link)

[21] D. W. Marques Guerra and T. Abrão, "RIS-aided System Channel Estimation using NN," in *Proc. of 2022 Symposium on Internet of Things (SIoT)*, pp.1-4, 2022. Article (CrossRef Link)

[22] S. Zeng, H. Zhang, B. Di, Z. Han and L. Song, "Reconfigurable Intelligent Surface (RIS) Assisted Wireless Coverage Extension: RIS Orientation and Location Optimization," *IEEE Communications Letters*, vol.25, no.1, pp.269-273, Jan. 2021. Article (CrossRef Link)

[23] N. Rajatheva et al., "White Paper on Broadband Connectivity in 6G," arXiv:2004.14247, 2020. Article (CrossRef Link)

[24] B. P. S. Sahoo, S. Narang, P. Jain, D. Kumar and S. K.Vankayala, "Mobility-aware Hybrid Channel Estimation Scheme for RIS-aided Millimeter-Wave Systems," in *Proc. of 2022 IEEE International Conference on Electronics, Computing and Communication Technologies (CONECCT)*, pp.1-5, 2022. Article (CrossRef Link)

[25] M. M. Amri, N. M. Tran, J. H. Park, D. I. Kim, and K. W. Choi, "Sparsity-Aware Channel Estimation for Fully Passive RIS-Based Wireless Communications: Theory to Experiments," *IEEE Internet of Things Journal*, vol.10, no.9, pp.8046-8067, May. 2023. Article (CrossRef Link)

[26] B. Zheng and R. Zhang, "Intelligent Reflecting Surface-Enhanced OFDM: Channel Estimation and Reflection Optimization," *IEEE Wireless Communications Letters*, vol.9, no.4, pp.518-522, Apr. 2020. Article (CrossRef Link)

[27] N. Varshney and S. De, "AoA-Based Low Complexity Beamforming for Aerial RIS Assisted Communications at mmWaves," *IEEE Communications Letters*, vol.27, no.6, pp.1545-1549, Jun. 2023. Article (CrossRef Link)

[28] J. Dai, Y. Wang, C. Pan, K. Zhi, H. Ren and K. Wang, "Reconfigurable Intelligent Surface Aided Massive MIMO Systems With Low-Resolution DACs," *IEEE Communications Letters*, vol.25, no.9, pp.3124-3128, 2021. Article(CrossRef Link)

[29] J. Dai, F. Zhu, C. Pan, H. Ren and K. Wang, "Statistical CSI-Based Transmission Design for Reconfigurable Intelligent Surface-Aided Massive MIMO Systems With Hardware Impairments," *IEEE Wireless Communications Letters*, vol.11, no.1, pp.38-42, Jan. 2022. Article(CrossRef Link)

[30] S. O. Mohammad T and E. T. Hamed, "The New Spectral Conjugate Gradient Method for Minimization," in *Proc. of 2022 International Conference on Data Science and Intelligent Computing (ICDSIC)*, pp.273-277, 2022. Article (CrossRef Link)

[31] V. Golovko, E. Mikhno, A. Kroschanka, M. Chodyka and P. Lichograj, "Adaptive Learning Rate for Unsupervised Learning of Deep Neural Networks," in *Proc. of 2023 International Joint Conference on Neural Networks (IJCNN)*, pp.1-6, 2023. Article (CrossRef Link)

[32] R. Jiang, X. Wang, S. Cao, J. Zhao and X. Li, "Joint Compressed Sensing and Enhanced Whale Optimization Algorithm for Pilot Allocation in Underwater Acoustic OFDM Systems," *IEEE Access*, vol.7, pp.95779-95796, 2019. Article (CrossRef Link)

[33] H. Yang, R. Fan, J. Chen and M. Xu, "Recurrent Neural Networks with Fractional Order Gradient Method," in *Proc. of 2022 14th International Conference on Advanced Computational Intelligence (ICACI)*, pp.49-55, 2022. Article (CrossRef Link)

[34] R. Jiang, Z. Fei, S. Huang, X. Wang, Q. Wu, and S. Ren, "Bivariate Pilot Optimization for Compressed Channel Estimation in RIS-Assisted Multiuser MISO-OFDM Systems," *IEEE Transactions on Vehicular Technology*, vol.72, no.7, pp.9115-9130, Jul. 2023. Article (CrossRef Link)

Xuemei Bai received her Ph.D. degree from Changchun University of Science and Technology, China, in 2009. She is currently a professor in the School of Electronic Information Engineering, Changchun University of Science and Technology. Her current research interests include intelligent information processing and pattern recognition.

Congcong Hou is currently working towards her master degree at Changchun University of Science and Technology within the school of Electronic Information Engineering. Her research interest includes signal and information Processing.

Chenjie Zhang received her master's degree from Changchun University of Science and Technology in 2008. She is currently an associate professor in the School of Electronic Information Engineering, Changchun University of Science and Technology. Her current research interests include intelligent information processing and pattern recognition.

Hanping Hu received his Ph.D.degree from Changchun Institute of Optics, Fine Mechanics and Physics, Chinese Academy of Sciences, China, in 2015. He is a laboratory teacher in the Schoolof Computer Science and Technology, Changchun University of Scence and Technology. His current research interests include deep learning and pattern recognition.